

Dual Faced Voltage Controlled Oscillator for Milli-Meter Wave Applications

A. Sunanda*, K. Suganthi**, S. Malarvizhi***

ABSTRACT

The voltage range of integrated oscillators will be more than required due to operation and temperature variations, which will lead to phase-noise. In this paper a dual-mode LC-tank generated VCO contains active core reconfiguration is constructed to allow two distinct modes of operation, with different oscillation frequencies which reduces phase noise with increased tuning ranges of 28%. The design is implemented in a 180nm CMOS technology and simulated using Advanced Design System tool, with measured tuning ranges of 59.5 GHz to 67.4 GHz, and 67.6 GHz to 77.3 GHz in the two modes respectively. This design ensures the overlapping of two oscillation mode frequency shades to degrade individual frequency span phase noise problem. This design is very useful and recommended for radar applications.

Index Terms: Dual-faced Oscillator, Phase Noise, voltage range, inductor, VCO, Recon figurable,

1. INTRODUCTION

An unexceptional methodology for intensifying oscillator tuning-range involves the use of a bank of tunable capacitors within the tank of inductor based oscillator. However, the phase-noise performance degrades as voltage range is increased, because of trade-off between key on-state resistance and parasitic capacitance. A resembled drawback is observed when using varactors for frequency adjusting. This paper describes an oscillator that works on active core reconfiguration [1], for milli-meter-wave applications. The implementation of this active core reconfiguration allows switching of oscillator operation, with different oscillation frequencies, by effectively modifying the inductance of an LC tank. As conferred below, the switches used for re-configuration do not contribute to tank loss. Fine frequency tuning is implemented using varactors in each switching. The model pursues to fortify co-occurring frequency spans in the couple of oscillation modes, such that the up-front end of the span of the low-frequency mode co-occurring with the lower end of the span of the high-frequency mode. This encompass the effective span of the oscillator. Since the frequency span required in each mode is compressed; the concession between voltage range and phase noise for varactor-based tuning is placid. Two or more distinct oscillators can also be used to alleviate this drawback. However the use of hyper-active core reconfiguration is expected to reduce the prospective for variations and mismatches that can arise from the use of two separate oscillators, since these would require individual self LC tanks that are physically apart on the IC, and require distinct path to the circuit given by the oscillators. The framework employed here is similar to [2]. However no implementation and measurements were included in [1]. This work also works as a customized spiral inductor or reducing die area. Apart to this work, the active core reconfiguration shown in [3] was employed to produce two huge separated frequencies. Switching that employ different architectures include [5] and [4], that effectively shift mutual inductance of multiple inductors to implement key mode oscillators; a triple band oscillator with active core switching [5]; and a mode switching oscillator based on switching capacitance [6]. The

* M.Tech (VLSI Design), SRM University.

** Assistant Professor, SRM University.

*** Professor, SRM University.

minimum size of the switches that is required to ensure transition from one mode to another is also analyzed. It is important to reduce switch size, since this helps to degrade the associated capacitive parasitic.

2. SWITCHING MODE VCO

The proposed switching mode VCO Fig. 1 consists an NMOS cross-coupled core that is partitioned into two identical parts. The LC tank consists of an inductor composed of sections L1, L2 and L3. The mutual inductance in these inductors initially avoided as shown in [7], The oscillator is portable in one of two modes through the use of switches SW1 and SW2. In one of the switching SW1 is OFF and SW2 is ON Fig. 2. In this mode, the voltages at both sides are identical to each other so that L1 current will pass and avoids over all inductance. The contour can be represented by two similar LC based VCOs in parallel, with an effective tank inductance

$$L_L = L2 + L3.$$

If the capacitance within each sectioned core is given by C, then the center frequency of oscillation will be

$$\omega_L = 1/2(L3 + L2)C$$

represented as common-mode (CM) configuration. In the second mode, SW1 is ON and SW2 is OFF (Fig.1c). The current flowing is 180° out of phase with the same magnitudes, placing an ac ground in the middle of the L1 sections. The effective inductance in this mode will be

$$L_H = (L_1 - L_2) + L3$$

with a corresponding oscillation frequency of

$$\omega_H = \frac{1}{2} \{(L1 - L2) + L3\}C$$

represented as differential-mode(DM) configuration. The ratio of the oscillation frequencies in the two modes is given by

$$\frac{W_L}{W_H} = \frac{(L_1 - L_2) + L_3}{L_2 + L_3}$$

Through proper scaling of inductors, a rigorous ratio between ωL and ωH can be achieved. Since in either mode the voltage across the switch terminals is similar, the key do not bequeath to the tank loss

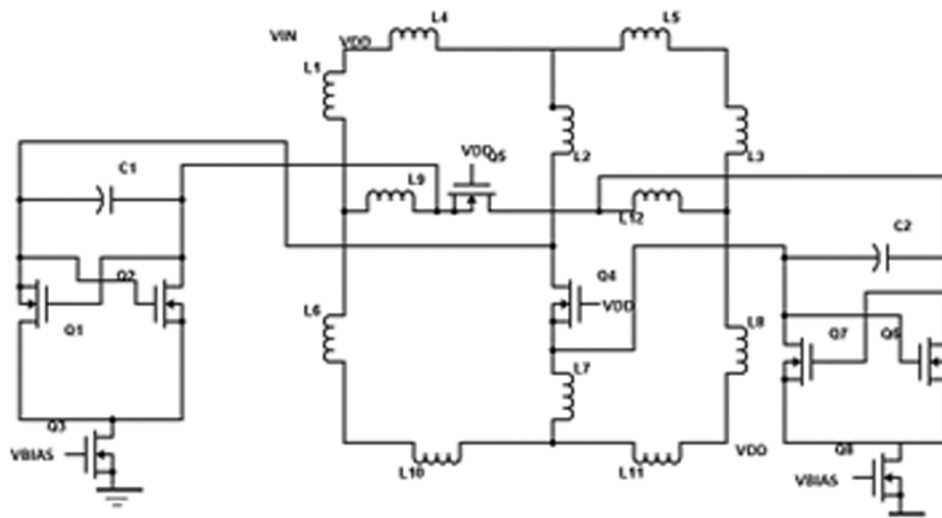


Figure 1: Common Mode operation of vco

[3]. Under the imagination that the impact of mutual inductance is ignored. The required tuning range around the formal frequency can be split into two overlapping halves. Then the tuning required per mode is also nearly divided, which relaxes the voltage-range vs. phase noise trade-off. It is also east to place a capacitor bank along with the varactor, in order to reduce the VCO gain (KVCO), which helps to enhance the phase noise.

3. DESIGN CONSIDERATION

The low frequency flicker noise degrades the phase noise due to the flicker noise is heterodyned to the oscillator output frequency due to the hyper active devices non-linear transfer function. The effect of flicker noise can be reduced with negative feedback that linearizes the transfer function is

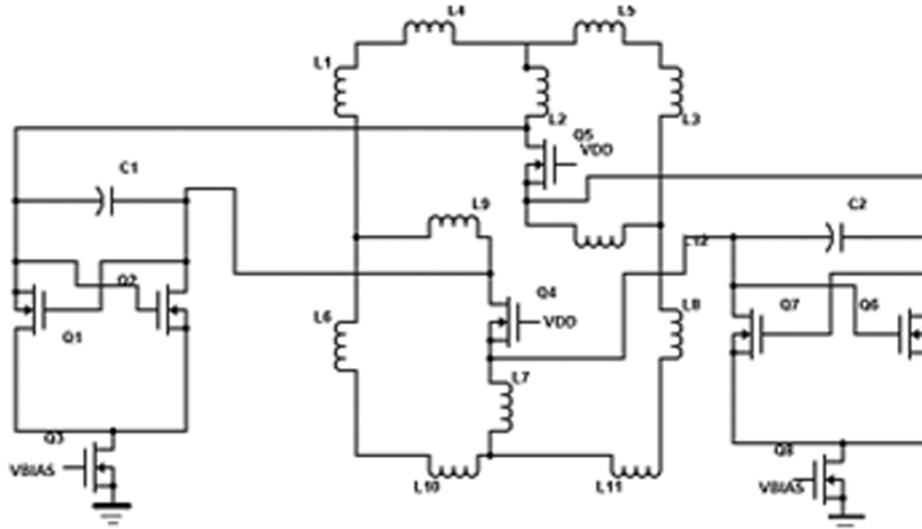


Figure 2: Differential Mode of VCO.

$$H(f) = \frac{K}{C_{ox} W_L f}$$

where K is the process-dependent constant, C_{ox} is the oxide capacitance in transistor devices, W and L are channel width and length respectively. The instantaneous frequency of a switching VCO is often modelled as a linear relationship with its instantaneous control voltage

$$f(t) = f_{0+K_0} V_{in}(t)$$

$$\theta(t) = \int_{-a}^t f(t) dt$$

$f(t)$ is the instantaneous frequency of the oscillator at time t, f_0 is the quiescent frequency of the oscillator K_0 is called the oscillator sensitivity, or gain. Its units are hertz per volt. $f(t)$ is the VCO's frequency $\theta(t)$ is the VCO's output phase.

3.1. Switching Mode Analysis

For analysing the resistor values designed in the circuit we have to calculate the approximate resistor values by

$$\frac{1}{R_L} = \frac{1}{R_{L,ind}} + \frac{1}{R_{L,cap}}$$

$$\frac{1}{R_H} = \frac{1}{R_{H,ind}} + \frac{1}{R_{H,cap}}$$

The switching analysis of VCO will form losses in inductors and capacitors which are represented by R_L, R_H . Where R_H^1, R_L^1 are the losses of capacitors and resistors in differential switching

$$\frac{1}{R_L^1} = \frac{1}{R_{L,ind}} + \frac{1}{R_{L,cap}} + \frac{2}{R_d}$$

$$\frac{1}{R_H^1} = \frac{1}{R_{H,ind}} + \frac{1}{R_{H,cap}} + \frac{2}{R_c}$$

The current which will pass into inductor & voltage across capacitor in high frequency mode i.e differential switching is

$$\frac{d}{dt}(2c.v_L) = -i_L - F_L - \frac{V_L}{R_L}$$

$$L_L \cdot \frac{d}{dt} i_L =$$

$$\frac{d}{dt}(2c.v_H) = -i_H - F_H - \frac{V_H}{R_H}$$

$$L_H \cdot \frac{d}{dt} i_H = V_H$$

By the vander val approximation the common mode and differential mode switching state equations of amplitude is measured as

$$\frac{d}{dt} A^2 L = \frac{a_1 - \left(\frac{1}{R_C}\right)}{2C} \cdot A^2 L - \frac{3 a_3}{8 C} \cdot A^4 L - \frac{3 a_3}{4 c} \cdot A^2 L \cdot A^2 H$$

$$\frac{d}{dt} A^2 H = \frac{a_1 - \left(\frac{1}{R_C}\right)}{2C} \cdot A^2 H - \frac{3 a_3}{8 C} \cdot A^4 H - \frac{3 a_3}{4 c} \cdot A^2 L \cdot A^2 H$$

3.1.1. Common-Mode to Differential-Mode Switching

In constant-state CM operation, with first switch OFF and SW2ON, the LHS is zero and AH = 0. Thus

$$\begin{aligned} 0 &= \frac{a_1 - (1 \div RH) \cdot A^2 H}{2c} - \frac{3 a_3}{8 c} \cdot A^4 H - \frac{3 a_3}{4 c} \cdot AL^2 \cdot AH^2 \\ &= 4 \left(a_1 - \frac{1}{RH} \right) - 3a_3 \cdot A^2 H - 6a_3 \cdot AL^2 \\ &= \left(a_1 - \frac{1}{RH} \right) - \frac{3}{4} \cdot a_3 \cdot AH^2 - \frac{3}{2} \cdot a_3 \cdot A^2 L > 0 \end{aligned}$$

$$= R_d < \frac{4}{a_1 + \frac{1}{R_H} - \frac{2}{R_L}}$$

Where R_d is the on-resistance of the differential switching

3.2. Differential-Mode to Common-Mode Switching

$$\begin{aligned} 0 &= \frac{a1 - (1 \div RL) \cdot A^2 L}{2c} - \frac{3}{8} \cdot \frac{a3}{c} \cdot A^4 L - \frac{3}{4} \cdot \frac{a3}{c} \cdot AL^2 \cdot AH^2 \\ &= 4(a1 - (1 \div RL)) AL^2 - 3(a3) AL^4 \\ &= 4 a1 AL^2 - 4(1 \div RL) AL^2 - 3a3 AL^4 \\ &= 4a1 - 4(1 \div RL) = 3a3 AL^2 \\ &= 4(a1 - (1 \div RL)) = 3a3 AL^2 \\ &= a1 - (1 \div RL) = \frac{3}{4} a3 \cdot AL^2 \\ &= a1 - \frac{1}{RH} - \frac{3}{4} a3 \cdot AH^2 - \frac{3}{2} a3 \cdot AL^2 > 0 \\ &= R_c < \frac{4}{a_1 + \frac{1}{R_H} - \frac{2}{R_L}} \end{aligned}$$

- Where AL = Amplitude of the low frequency mode
 AH = Amplitude of the high frequency mode
 RL = Total shunt losses of the low frequency mode
 RH = Total shunt losses of the high frequency mode
 Rd = On resistance of the differential mode
 Rc = On resistance of the common mode

3.3. Phase noise Calculations

By leasons phase noise equation we can calculate average phase noise generated in the oscillator with its specific requirements

$$(\Delta w) = 10 \log \left(\frac{2KFT}{P_s} \right) * \left(\frac{W_0}{2\theta \Delta w} \right)^2$$

- F = empirical parameter
 K = Boltzmann's constant
 T = absolute temperature
 P_s = average power dissipated at resistive part
 W_0 = oscillation frequency

Phase noise will be degraded by using reducing the resistors and capacitors in the schematic diagram

4. SCHEMATIC TOPOLOGY OF SWITCHING VCO

Novality in this design is shown as the switching mode vco which is operated in two different modes where the frequency balancing is done using this unique kind of VCO, As one mode will give high frequency upto 75.3GHz and the former one will give the low frequency starting with 64.3GHz which will made the design flexibe to all robust conditions the execution of common mode configuration is shown in Fig. 3, as the schematic is modelled using ADS simulation The measured tuning range in the two modes is 59.5-67.4 GHz and 67.4-77.3 GHz.

The differential pair of transistors which is attached to the bulk of paired inductors with couple of capacitors is configured into common mode switching which is operated in low frequency i,e from ,The

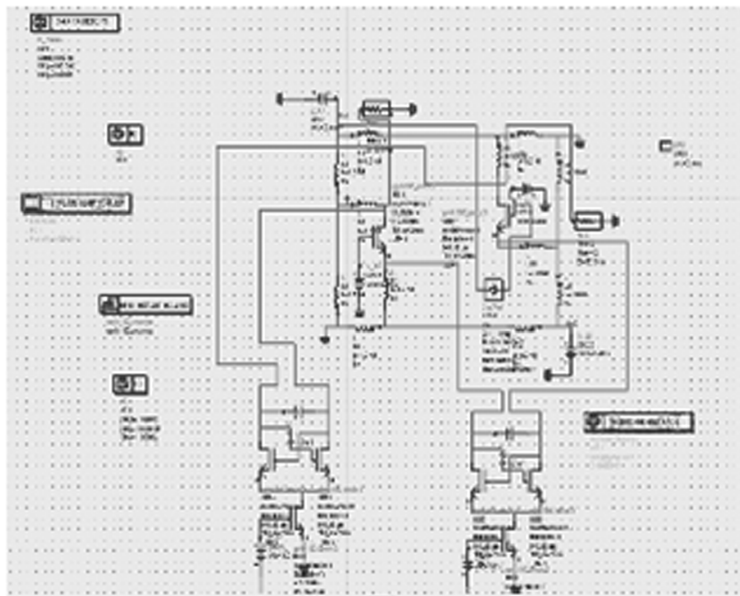


Figure 3: Common Mode Switching of VCO

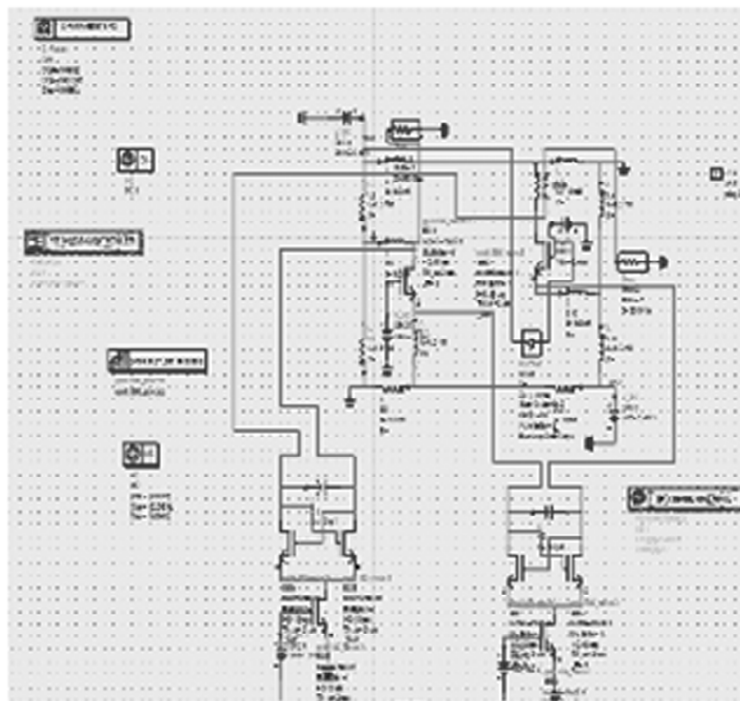


Figure 4: Differential Mode Switching VCO

Table 1
Tabular form of simulated results

Parameter	Value
NF	0.05dB
S_{11}	<-10dB
TECHNOLOGY	0.18 μ m
Power dissipation	5mW
Phase noise	-117dBc/Hz

oscillations with measured tuning range from 64.3 to 75.6GHz oscillation ports are placed at the two voltage biasing to measure the transient analysis of the schematic and also to evaluate the frequency variations, eliminating the phase noise by developing the immune noise figure which will avoid uncertain disturbances.

5. SIMULATION RESULTS

The oscillating frequency of the common mode and differential mode switching will varies according to the given Vdc, where the voltage controlled oscillator will generate noise free sine wave transient analysis

Transient analysis will show the oscillations of the switching mode VCO

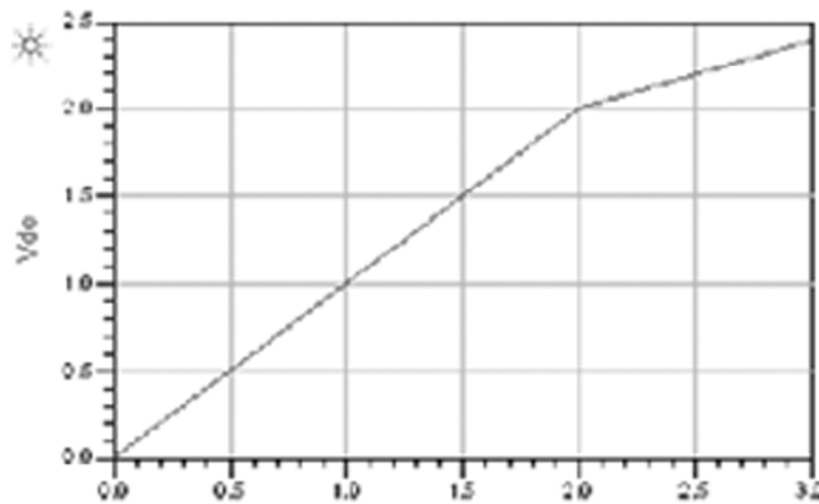


Figure 5: Variations of Frequency vs Bias voltage

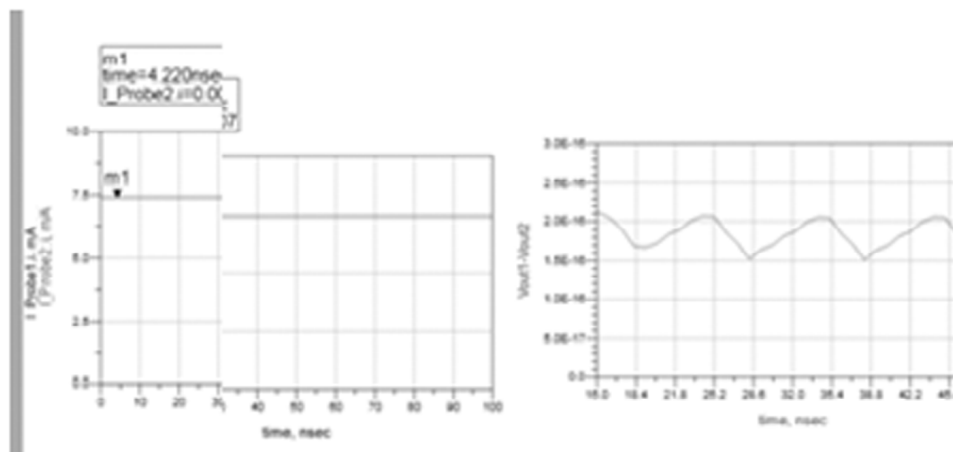


Figure 6: Transient Analysis of VCO

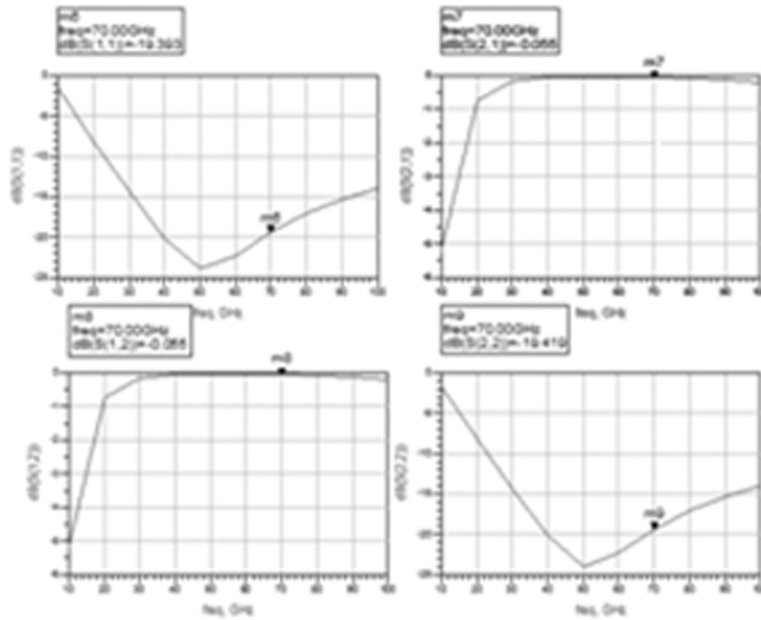


Figure 7: S-parameter Calculation of Proposed VCO

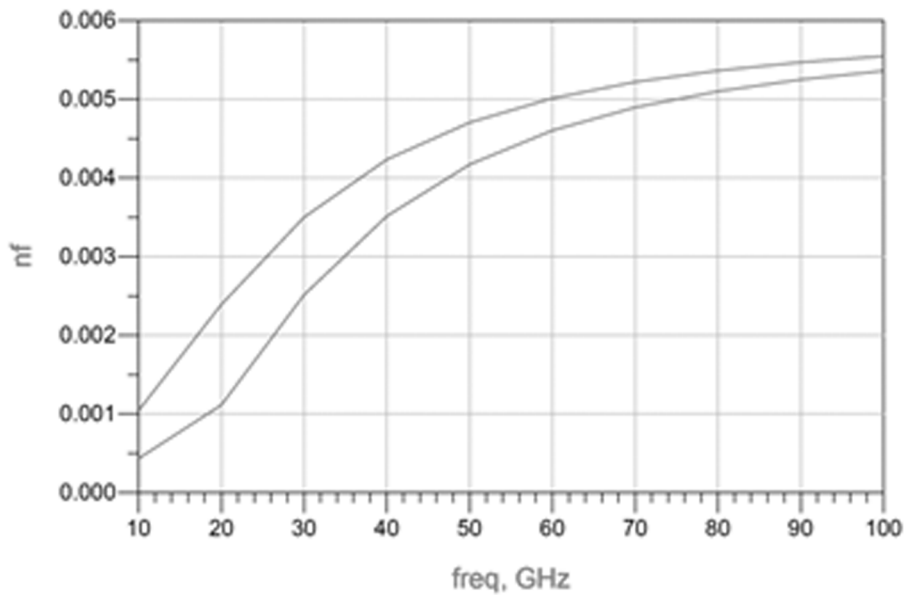


Figure 8: Noise Figure of VCO

The noise factor is the ratio of actual outcome noise to that which would stand if the device itself did not introduce noise, or the ratio of input SNR to output SNR. The s-paramters obtained using the proposed oscillator have matching between $S(1, 2)$, $S(2, 1)$ and the $S(1, 1)$ should be more than -10 dB.

The Noise Figure of the switching proposed VCO is 0.05dB shown in fig. 9 at the measured frequency of 67.8GHz where the noise is eliminated from the oscillator. The calculated DC power of the VCO core proscribed output buffers was 13 mW from a 2.5V supply, which is comparable to the state-of-the-art performance.

Phase noise centres around frequency stability, or the characteristic of an oscillator to produce the same frequency over a specified time period as in this switching mode VCO the measured frequency at 70GHz is -117dBc /Hz.

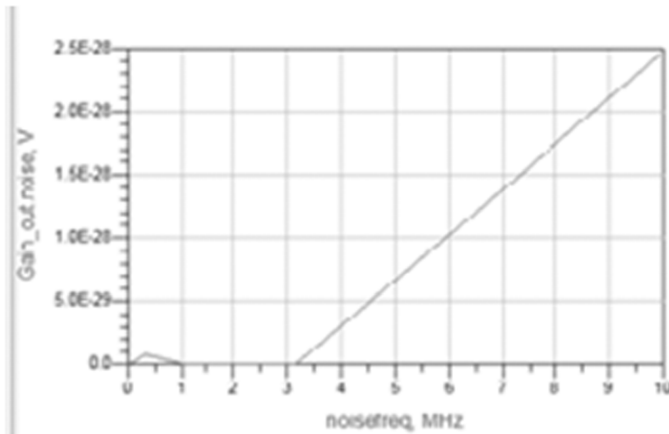


Figure 9: Phase Noise of switching mode VCO.

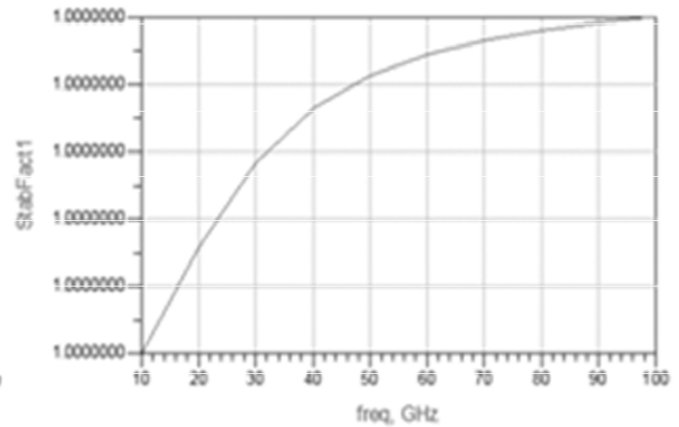


Figure 10: Loop Gain for the switching mode VCO.

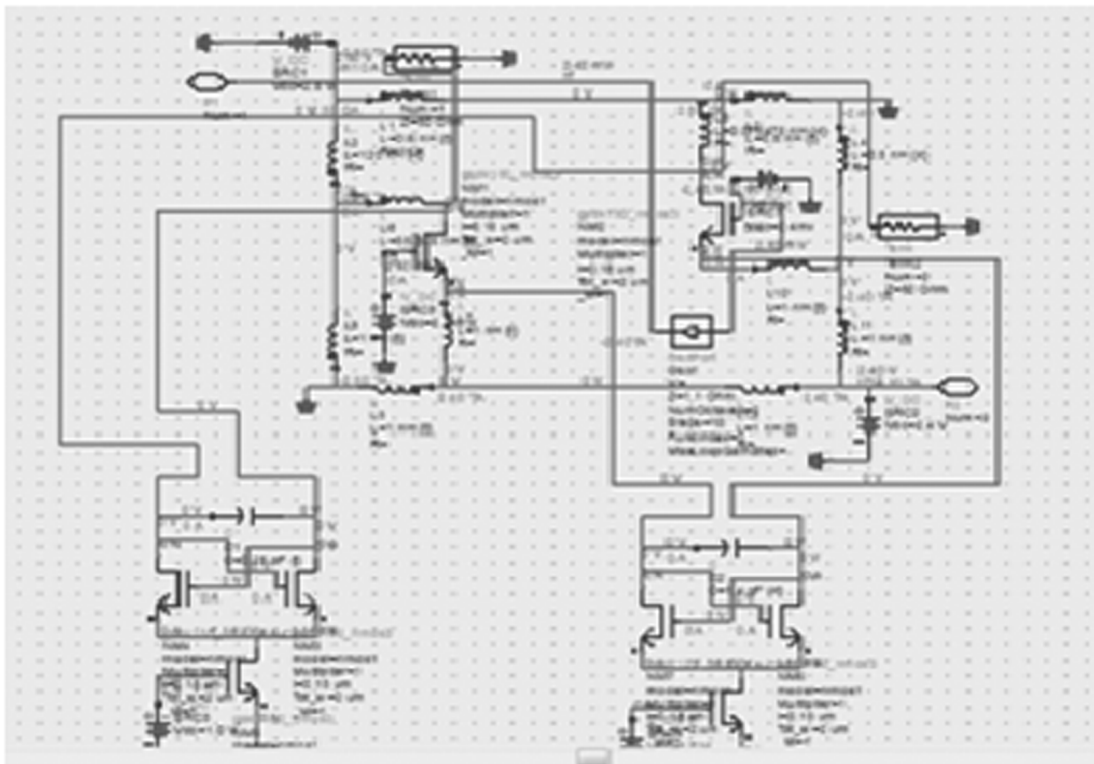


Figure 11: Power Dissipated across each Transistor

The Barkhausen stability paradigm is a mathematical condition to identify when a linear electronic circuit will oscillations where the loop gain is equal to unity in absolute magnitude which is shown in Fig. 10.

Power consumption of the circuit is 5mw which is much better than the existing oscillators ,as the above Fig. 11. shows the power dissipated across each transistor.

6. CONCLUSION

A switching mode reconfigurable VCO is demon-started here using 0.18um technology in ADS simulation. The large frequency span helps to mitigate the impact of variability, which can pose a sententious challenge in mm-wave designs. The phase noise is compressed even though at high frequency operation and a less distortion oscillations are generated with minute power consumption of 5mW.

REFERENCES

- [1] J. Kim and D. Peroulis, "Tunable MEMS spiral inductors with optimized RF performance and integrated large-displacement electrothermal actuators," *IEEE Trans. Microw. Theory Tech.*, vol. 57, no. 9, pp. 2276–2283, Sep. 2009.
- [2] N. H. W. Fong, J.O. Plouchart, N. Zamdmer, D. Liu, L. C. Plett, and N. G. Tarr, "Design of wide-band CMOS VCO for multiband wireless LAN applications," *IEEE J. Solid-State Circuits*, vol. 38, no. 8, pp. 1333–1342, Aug. 2003.
- [3] T. H. Lee and A. Hajimiri, "Oscillator phase noise: A tutorial," *IEEE J. Solid-State Circuits*, vol. 35, no. 3, pp. 326–336, Mar. 2000.
- [4] C. Cao and K. K. O, "Millimeter-wave voltage-controlled oscillators in 0.13- μm technology," *IEEE J. Solid-State Circuits*, vol. 41, no. 6, pp. 1297–1304, Jun. 2006.
- [5] T.L. Hsieh et al., "A reconfigurable oscillator topology for dual-band operation," in Proc. IEEE Int. Conf. on VLSI Design, 2005, pp. 870–873.
- [6] R. Gharpurey et al., "A single-tank dual-band reconfigurable oscillator," in Proc. IEEE Symp. on VLSI Ckts, 2006, pp. 176–177.
- [7] S. Agarwal et al., "A dual-mode wide-band MOS oscillator," in Proc. IEEE DCAS, 2009, pp. 1–3.
- [8] A. Bevilacqua et al., "Transformer-based dual-mode voltage-controlled oscillators," *IEEE TCAS II*, vol. 54, no. 4, pp. 293–297, 2007.
- [9] B. Razavi, "Multi-decade carrier generation for cognitive radios," in Proc. IEEE Symp. on VLSI Ckts, 2009, pp. 120–121.
- [10] Z. Safarian et al., "A 1.3–6 GHz triple-mode CMOS VCO using coupled inductors," in Proc. IEEE CICC, 2008, pp. 69–72.
- [11] G. Li et al., "A distributed dual-band LC oscillator based on mode switching," *IEEE T-MTT*, vol. 59, no. 1, pp. 99–107, 2011.
- [12] A. Goel et al., "Frequency switching in dual-resonance oscillators," *IEEE JSSC*, vol. 42, no. 3, pp. 571–582, 2007.
- [13] D. Ghosh et al., "Evolution of oscillation in a quadrature oscillator," in Proc. IEEE Int. Conf. on VLSI Design, 2011, pp. 36–40.
- [14] A. Jooyaie et al., "A V-band voltage controlled oscillator with greater than 18 GHz of continuous tuning-range based on orthogonal E mode and H mode control," in Proc. IEEE RFIC Symp., 2011.